

Effects of Electrochemical Parameters on the Electropolymerisation of 2-nitro-p-phenylenediamine in Caustic and Neutral Solutions

Mohammad A. Kanan^{1,*}, and Ahmad S. Barham²

¹ Industrial Engineering Department, College of Engineering (CE), University of Business and Technology (UBT), Jeddah 21448, Kingdom of Saudi Arabia

² General Subjects Department, College of Engineering (CE), University of Business and Technology (UBT), Jeddah 21448, Kingdom of Saudi Arabia

*E-mail: m.kanan@ubt.edu.sa

Received: 4 January 2020 / Accepted: 28 February 2020 / Published: 10 April 2020

A thin film of poly (2-nitro-p-phenylenediamine) (2NPPD) was prepared by electrochemical means of cyclic voltammetric technique. The films were deposited on 1.6 mm diameter gold electrodes ($A=0.0201\text{ cm}^2$) or 3.0 mm glassy carbon ($A=0.0707\text{ cm}^2$). We electrochemically investigated 2NPPD monomer in either a caustic solution of 10 mmol dm^{-3} sodium hydroxide (pH 9.2) or a neutral solution (pH 7.0) contained 0.1 mol dm^{-3} KCl. A general factorial design was constructed to study the electropolymerisation development of poly 2NPPD by tracking the interactions between the factors of scan rates and the electrode's material types. In the general factorial design, the response was chosen to be the first anodic current peak densities obtained from the CVs in triplicates. In all CV measurements, the rapid drop in the anodic current was highlighted as an indication of electropolymerisation. We obtained good passivation of the poly 2NPPD for the modified electrodes prepared from the neutral medium and caustic aqueous solutions at slower scan rates. At faster scan rates, poor passivation of the modified surfaces was observed, possibly attributed to the thickness of the poly 2NPPD formed and hence the amount of the polymer deposited on the surfaces. Morphological features of poly 2NPPD were inspected using scanning electron microscopy. The diffusion coefficients were measured using the Randles–Sevcik equation and confirmed that the electropolymerisation of 2NPPD monomer is a linear diffusion-controlled process.

Keywords: Electropolymerisation; Poly (2-nitro-p-phenylenediamine); General Factorial Design; Electrochemical Cyclic Voltammetry (CV); Diffusion.

1. INTRODUCTION

Electropolymerisation is a coating process wherein the polymer is deposited from a monomer solution onto a substrate. This method of coating is frequently applied to coat relatively small parts or

zones on the substrate's surface. Experimental parameters of electropolymerisation are the current and the applied potential, and the magnitude of the latter should be sufficient to polymerise the monomer. The solubility of the monomer should also be sufficient to allow the monomer to dissolve in the selected solvent along with a necessary supporting electrolyte. All these ingredients will form the so-called polymerisation solution. The polymerisation solution is then transferred into an electrochemical cell consisting of three electrodes. The first electrode is the working electrode which is the substrate to be coated; the other two electrodes are made from inert materials, generally platinum (Pt) for the counter electrode and Ag/AgCl or SCE for the reference electrode [1-4].

Several researchers studied the electropolymerisation of nitroaniline and aniline derivatives [5-8]. Arjomandi et al. presented a novel conducting poly (*p*-nitroaniline-co-*N*-methylaniline) material, obtained by electro-copolymerisation of *para*-nitroaniline and *N*-methylaniline in aqueous sulfuric acid solution [6]. Electrosynthesis was carried out using cyclic voltammetry (CV) technique with different monomer feed concentrations [6]. Sağlam et al. developed a novel electrochemical sensor for the detection of nitroaromatic explosive materials based on a gold nanoparticle-modified glassy carbon electrode coated with poly(*o*-phenylenediamine–aniline film) [5]. Shumyantseva et al. examined the electrosynthesis of molecularly imprinted polymer templated with myoglobin; the reference non-imprinted polymer was with *o*-phenylenediamine as a monomer [7]. Poochai et al. fabricated a high-rate supercapacitor by co-electropolymerisation using different co-monomer feeding ratios in 0.5 M H₂SO₄ of hydrophilic poly(aniline-co-*p*-phenylenediamine) nanofiber-decorated nitrogen-doped reduced graphene oxide [8]. Ding et al. successfully copolymerised aniline with *m*-nitroaniline. Moreover, *m*-nitroaniline could polymerise on a polyaniline-modified electrode to generate the polyaniline/poly(*m*-nitroaniline) composite using potential cycling. Poly (aniline-co-*m*-nitroaniline) could be readily synthesised in various molar ratios of co-monomers by chemical and electrochemical polymerisation [9]. Chemchoub et al. modified by electropolymerisation a carbon paste electrode of poly-(*para*-phenylenediamine) via CV. At a constant potential, they electrodeposited Nickel particles on the polymer film. They found that the poly-(*para*-phenylenediamine) and Ni particles to be a promising non-precious electrocatalyst, which might be utilised efficiently to enhance the performance of direct methanol fuel cells [10].

In cosmetics and personal care products, 2-Nitro-*p*-phenylenediamine (2NPPD) – a reddish-brown crystalline powder – has been used in hair dyes formulations, tints and colours, as well as widely used as a non-oxidative coal-tar dye in semi-permanent or oxidative permanent tinting colour. It is not an oxidation dye but is present in oxidation formulations as a colour tinting agent.

The current researchers conducted a comprehensive electrochemical study to enrich our knowledge regarding the electrochemical properties of 2NPPD and because our compound has not been extensively studied in the literature. Consequently, this paper examines the electrochemical parameters of 2-nitro-*p*-phenylenediamine by CV prepared in basic and neutral solutions through a general factorial design. The design aimed to investigate the electrochemical parameters of the electropolymerisation process, such as scan rates and the electrode's material types. Morphology of the obtained thin film polymers was shown.

2. EXPERIMENT

2.1. Materials and reagents

All chemicals were used as received. 2-Nitro-P-Phenylenediamine (2NPPD), potassium ferricyanide (>98%), potassium ferrocyanide trihydrate (>98%), and potassium chloride (99%), were all purchased from Alfa Aesar, Germany. Sodium hydroxide (98%) was procured from PRS, Panreac, Spain. All aqueous solutions were prepared using deionised water from a Milli-pore Milli-Q system (resistivity=18.2 M Ω cm).

2.2. Film Preparation

The current work used an EZstat-Pro potentiostat equipped with an EZware 2013 V7 analysing software and a three-electrode glass cell throughout (NuVant Systems Inc. (IN, USA)).

The first step was polishing and cleaning the working electrode (gold or glassy carbon) to ensure decent electron transfer. The polishing/cleaning process was conducted mechanically for two minutes using the suspended solution of 0.05 μm alumina performed on polishing pads (polishing kit number: PK-4) purchased from BASi Preclinical Services (IN, USA). The working electrode was immediately flushed with excess deionised water to remove any remaining alumina deposits.

We conducted a voltammogram run of 20.0 mmol dm^{-3} $\text{K}_3\text{Fe}(\text{CN})_6/\text{K}_4\text{Fe}(\text{CN})_6$ consisting of 0.1 mol dm^{-3} KCl electrolyte versus Ag/AgCl (3.0 mol dm^{-3} KCl) between -0.2 V and 0.6 V at a sweep rate of 20 mV s^{-1} for six sweeps of applied potential to test the polished working electrodes.

The counter electrode used was a platinum coiled wire (230 mm) mounted in a CTFE[®] cylinder. The reference electrode used was Ag/AgCl (3.0 mol dm^{-3} KCl). All electrodes used in this study were supplied by BASi (IN, USA).

In the current study, 2NPPD monomer was electropolymerised using 1.6 mm diameter gold electrodes ($A=0.0201 \text{ cm}^2$) or 3.0 mm glassy carbon ($A=0.0707 \text{ cm}^2$). The concentration of the 2NPPD monomer of 10.0 mmol dm^{-3} was prepared separately by using either 0.1 mol dm^{-3} KCl (neutral solution), or caustic solution of 10 mmol dm^{-3} sodium hydroxide. Next, runs of voltammograms of 2NPPD solutions versus Ag/AgCl (3.0 mol dm^{-3} KCl) were conducted and the sweep ranged from 0.0 to 1.0 V for different sweep rates: $v = 5 \text{ mV/s}$, 10 mV/s , 15 mV/s , 20 mV/s , 25 mV/s , and 30 mV/s . Therefore, electropolymerisation was performed by using CV in the mentioned potential region using 20 cycles. Polymer film deposition was verified by testing all the modified electrodes in 20.0 mmol dm^{-3} $\text{K}_3\text{Fe}(\text{CN})_6/\text{K}_4\text{Fe}(\text{CN})_6$ consisting of 0.1 mol dm^{-3} KCl versus (Ag/AgCl, 3.0 mol dm^{-3} KCl) at a sweep rate of 20 mV s^{-1} for six sweeps of applied potential.

Gold-coated silicon wafer (Au.1000.SL1) with a layer of 100 nm gold and 5.0 nm titanium thicknesses was purchased from Platypus Technologies, Madison, USA. The gold-coated Si wafer was cut into small 1.0 $\text{cm}\times 1.0 \text{ cm}$ chips using LatticeAx[™] 120, LatticeGear, USA and used as working electrodes in the electropolymerisation of 2NPPD as described above in the film preparation section. The surface morphology of the modified electrodes of gold-coated Si-chips ($A=1.0 \text{ cm}^2$) was analysed by scanning electron microscopy using an ULTRA 55 ZEISS (Germany). Before SEM capturing, the

samples were mounted on metallic stubs with double-sided adhesive tape. The SEM was operated at an accelerating voltage of 6 kV, high-efficiency In-lens SE detector, and a working distance of 5.0 mm.

2.3. Design of experiments (DOE) construction and evaluation

We constructed a general factorial design of experiments to explore the interactions between the operating parameters on the electropolymerisation of 2NPPD prepared in a neutral medium. Scan rate and the electrode's material types were selected to investigate their effects on the electropolymerisation process using CV. The selected response was the first anodic peak current densities obtained from the first CV cycle in each run. These responses were analysed using Design Expert 7.0.0. (Stat-Ease, Inc., USA). Moreover, we performed each run in triplicate in order to ensure reproducibility.

Table 1 presents the general factorial matrix along with the output values of each run. The first factor is the scan rate. Six levels of scan rates were used: 5, 10, 15, 20, 25, and 30 mV/s. Two levels of the second factor of gold and glassy carbon signified the electrode's materials. Tables 2 and 3 present the levels of the design study under question.

Table 1. Experimental data along with standard order and run as per DOE matrix

Standard order	Run	Factor 1: Scan Rate (mV)	Factor 2: Electrode's Type	Response: First anodic peak current density ($\mu\text{A}/\text{cm}^2$)
27	1	15	GC	296
28	2	20	GC	344
15	3	25	G	403
14	4	25	G	379
22	5	10	GC	236
6	6	10	G	243
7	7	15	G	323
34	8	30	GC	413
8	9	15	G	318
12	10	20	G	363
33	11	25	GC	390
35	12	30	GC	429
31	13	25	GC	396
18	14	30	G	507
25	15	15	GC	289
21	16	5	GC	149
20	17	5	GC	135
24	18	10	GC	228

23	19	10	GC	218
30	20	20	GC	335
9	21	15	G	303
5	22	10	G	263
4	23	10	G	282
32	24	25	GC	400
26	25	15	GC	300
13	26	25	G	414
3	27	5	G	181
16	28	30	G	406
29	29	20	GC	338
2	30	5	G	191
17	31	30	G	470
11	32	20	G	408
1	33	5	G	208
19	34	5	GC	146
36	35	30	GC	417
10	36	20	G	342

Table 2. Factors of scan rate and factor levels (Number of levels: 6)

Scan Rate (mV/s)	A[1]	A[2]	A[3]	A[4]	A[5]
5	1	0	0	0	0
10	0	1	0	0	0
15	0	0	1	0	0
20	0	0	0	1	0
25	0	0	0	0	1
30	-1	-1	-1	-1	-1

Table 3. Factors of the electrode's material types and factor levels (Number of levels: 2)

Electrode's Type	B[1]
Gold (G)	-1
Glassy Carbon (GC)	1

3. RESULTS AND DISCUSSION

Figure 1A and Figure 1B present the CV curves related to the electropolymerisation of 10 mmol dm⁻³ 2-nitro-p-phenylenediamine (2NPPD) using bare 1.6 mm gold electrodes ($A=0.0201\text{ cm}^2$) and bare

3.0 mm glassy carbon electrodes ($A=0.0707\text{ cm}^2$), respectively. All potentials were measured versus Ag/AgCl (3.0 mol dm⁻³ KCl). 2NPPD monomer was prepared in neutral aqueous solutions (pH=7.0). The figures illustrate the first and second sweeps for every scan rate used ranging from 5 up to 30 mV/s for 25 sweeps.

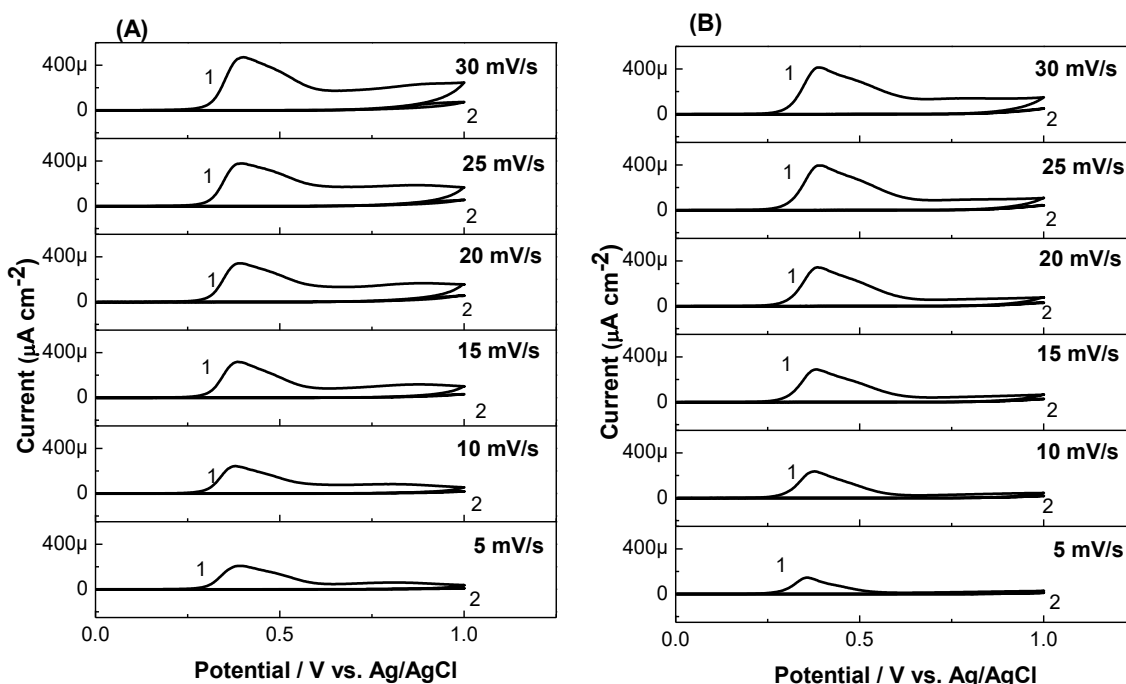


Figure 1. Electropolymerisation in neutral solutions at pH=7.0 (0.1 mol dm⁻³ KCl) of 10.0 mmol dm⁻³ 2-nitro-p-phenylenediamine (2NPPD) vs Ag/AgCl (3.0 mol dm⁻³ KCl). Cyclic voltammograms obtained at a scan rate of 5 up to 30 mV s⁻¹ (25 cycles). All measurements were performed on a (A) bare 1.6 mm gold electrode ($A=0.0201\text{ cm}^2$) and (B) bare 3.0 mm glassy carbon electrode ($A=0.0707\text{ cm}^2$). This figure reveals the first and second cycles for every scan rate.

In the first cycle of each scan rate, an anodic oxidation peak was observed at a range of 0.38 to 0.40 V (Figure 1A). Current densities of 207 $\mu\text{A}/\text{cm}^2$, 318 $\mu\text{A}/\text{cm}^2$, and 470 $\mu\text{A}/\text{cm}^2$ were obtained for the 5 mV, 15 mV, and 30 mV scan rate, respectively. However, in Figure 1B, the first cycle of each scan rate revealed an anodic oxidation peak at a range of 0.35 to 0.39 V. Current densities of 146 $\mu\text{A}/\text{cm}^2$, 289 $\mu\text{A}/\text{cm}^2$, and 412 $\mu\text{A}/\text{cm}^2$ were obtained for the 5 mV, 15 mV, and 30 mV scan rate, respectively.

A notable feature was observed in Figures 1A and 1B, namely an irreversible oxidation reaction obtained at both electrode surfaces. Additionally, the first anodic peak disappeared in subsequent cycles (from the second sweep onwards). These findings are in good agreement with the results obtained from Yu et al [11]. Yu et al. reported the anodic electropolymerization of 4-nitro-1,2-phenylenediamine (4NoPD) at different pH media [11]. They showed the feasibilities of forming poly (P4NoPD) on gold and glassy carbon electrodes. They generated the poly (P4NoPD) by continuous potential cycling between -0.15V and +1.10V (versus Ag/AgCl, saturated KCl). The amount of polymer deposited were found to influence strongly by the pH of the electropolymerization medium used. The attached nitro-groups have been greatly influenced also by pH. A single irreversible wave was observed at 0.15 V and

0.10 V at pH of 5.41 and 7.90, respectively [11]. These values were slightly smaller than our values presented in Figure 1.

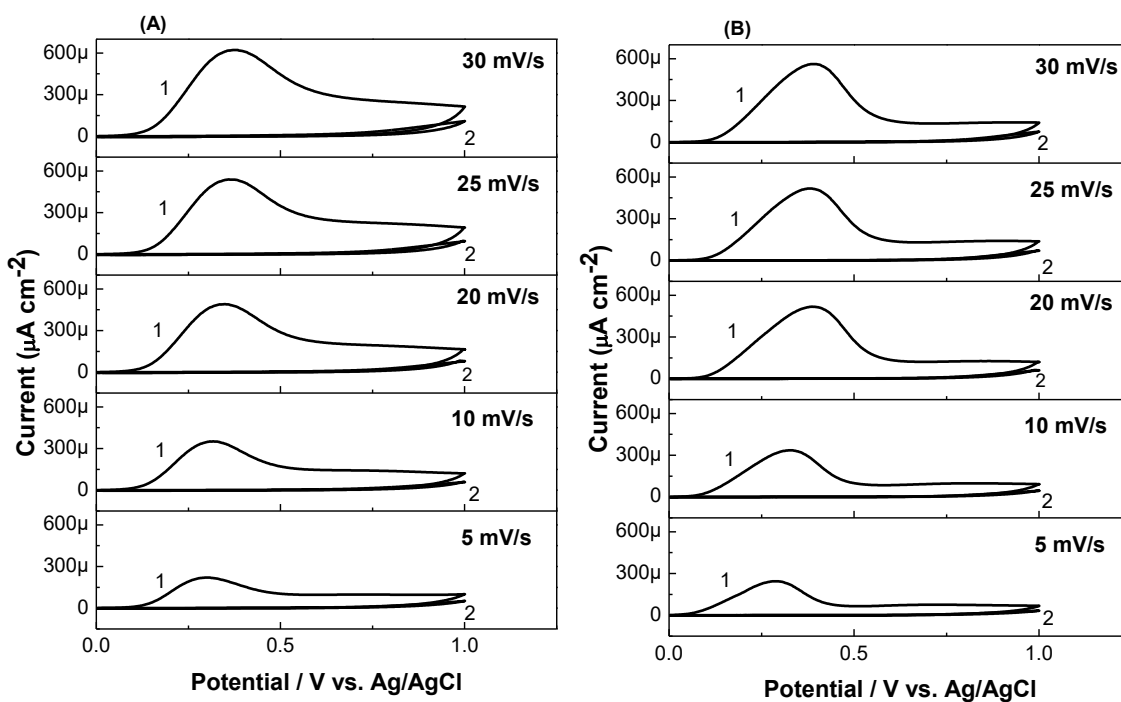


Figure 2. Electropolymerisation of 10.0 mol dm^{-3} 2NPPD vs Ag/AgCl (3.0 mol dm^{-3} KCl) in 10 mol dm^{-3} caustic sodium hydroxide solutions. Cyclic voltammograms were obtained at a scan rate of 5 up to 30 mV s^{-1} (25 cycles). All measurements were performed on a (A) bare 1.6 mm gold electrode ($A=0.0201 \text{ cm}^2$) and (B) bare 3.0 mm glassy carbon electrode ($A=0.0707 \text{ cm}^2$). This figure reveals the first and second cycles for every scan rate.

Figures 2A and 2B present the CV curves connected to the electropolymerisation of 10 mol dm^{-3} 2NPPD using gold electrodes and glassy carbon electrodes, respectively. 2NPPD monomer was prepared in 10 mol dm^{-3} NaOH caustic solution (pH=9.2). The figures show the first and second sweeps for every scan rate used ranging from 5 up to 30 mV/s for 25 sweeps.

We observed an anodic oxidation peak in the first cycle of each scan rate at a range of 0.30 to 0.38 V (Figure 2A). Current densities of $220 \text{ } \mu\text{A/cm}^2$, $489 \text{ } \mu\text{A/cm}^2$, and $622 \text{ } \mu\text{A/cm}^2$ were obtained for the 5 mV, 20 mV, and 30 mV scan rate, respectively. However, in Figure 2B, the first cycle of each scan rate revealed an anodic oxidation peak at a range of 0.29 to 0.39 V. Current densities of $244 \text{ } \mu\text{A/cm}^2$, $516 \text{ } \mu\text{A/cm}^2$, and $562 \text{ } \mu\text{A/cm}^2$ were obtained for the 5 mV, 20 mV, and 30 mV scan rate, respectively. A notable irreversible oxidation reaction obtained at both electrode surfaces was observed in Figures 2A and 2B. Furthermore, the first anodic peak disappeared in subsequent cycles. Sayyah et al. recorded the CV of 0.08 M *o*-phenylenediamine on Pt-electrode from deoxygenated solution containing 0.5 mol dm^{-3} HCl and 0.1 mol dm^{-3} Na_2SO_4 with scan rate of 25 mV s^{-1} [12]. A single irreversible wave was observed at approximately 0.60 V and the entire CV pattern was similar to the CVs presented in Figure 2.

Figure 3 presents the electrochemical behaviour for the bare electrodes of gold and glassy carbon tested in $20 \text{ mmol dm}^{-3} \text{ K}_3\text{Fe}(\text{CN})_6/\text{K}_4\text{Fe}(\text{CN})_6$ consisting of $0.1 \text{ mol dm}^{-3} \text{ KCl}$ versus Ag/AgCl ($3.0 \text{ mol dm}^{-3} \text{ KCl}$) at 20 mV s^{-1} (4 cycles). We observed oxidation peaks at $+270 \text{ mV}$ ($3.5 \times 10^{-3} \text{ mA cm}^{-2}$) and a reduction at $+181 \text{ mV}$ ($3.3 \times 10^{-3} \text{ mA cm}^{-2}$) for the bare gold electrode. For glassy carbon electrode, we observed the oxidation peak and the reduction peak at $+280 \text{ mV}$ ($3.1 \times 10^{-3} \text{ mA cm}^{-2}$) and $+176 \text{ mV}$ ($3.1 \times 10^{-3} \text{ mA cm}^{-2}$), respectively. These findings are in good agreement with our previous results [13-19].

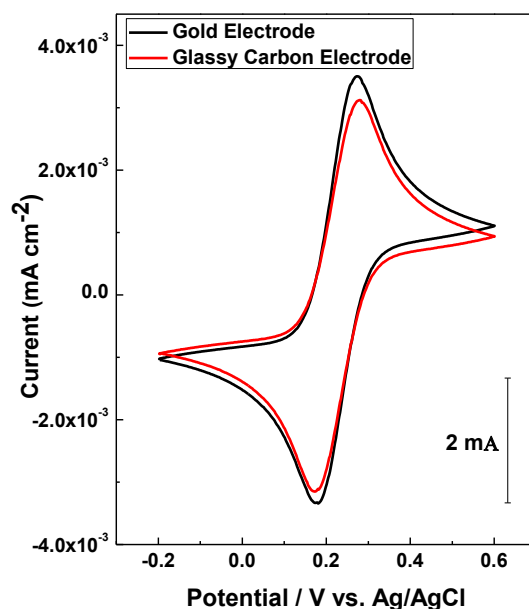


Figure 3. CV curves recorded for the bare electrodes using $20 \text{ mmol dm}^{-3} \text{ K}_3\text{Fe}(\text{CN})_6/\text{K}_4\text{Fe}(\text{CN})_6$ consisting of $0.1 \text{ mol dm}^{-3} \text{ KCl}$ vs Ag/AgCl ($3.0 \text{ mol dm}^{-3} \text{ KCl}$) at 20 mV s^{-1} (4 cycles). The CV curve for the bare gold electrode is presented in black ($A=0.0201 \text{ cm}^2$), and the bare glassy carbon electrode is presented in red ($A=0.0707 \text{ cm}^2$).

Figure 4 illustrates the results of the modified or blocked electrode obtained in Figure 1 following testing for passivation of the electrode's surfaces in $20.0 \text{ mmol dm}^{-3} \text{ K}_3\text{Fe}(\text{CN})_6/\text{K}_4\text{Fe}(\text{CN})_6$ consisting of $0.1 \text{ mol dm}^{-3} \text{ KCl}$ versus Ag/AgCl ($3.0 \text{ mol dm}^{-3} \text{ KCl}$) at 20 mV s^{-1} (4 sweeps) [15, 16, 20]. However, the CVs presented in Figure 4 were the test results for the modified electrodes in ferricyanide/ferrocyanide solutions. The modified electrodes were previously prepared in neutral aqueous solutions of $10.0 \text{ mmol dm}^{-3} \text{ 2NPPD}$ ($\text{pH}=7.0$) versus Ag/AgCl ($3.0 \text{ mol dm}^{-3} \text{ KCl}$) at $5\text{--}30 \text{ mV s}^{-1}$ scan rates. Then, we compared the results in Figure 4 with the same of the bare electrodes in Figure 3, the current peaks related to the bare electrodes diminished [15, 16].

All the modified electrodes used to construct Figure 2 have been tested for passivation of the electrode's surfaces by electropolymerisation in $20.0 \text{ mmol dm}^{-3} \text{ K}_3\text{Fe}(\text{CN})_6/\text{K}_4\text{Fe}(\text{CN})_6$ consisting of $0.1 \text{ mol dm}^{-3} \text{ KCl}$ versus Ag/AgCl ($3.0 \text{ mol dm}^{-3} \text{ KCl}$) at 20 mV s^{-1} (4 sweeps) [19]. Figure 5 presents

the CV results. The concentration of 2NPPD monomer was $10.0 \text{ mmol dm}^{-3}$ and was electropolymerised in 10 mmol dm^{-3} NaOH caustic solution at pH=9.2 versus Ag/AgCl (3.0 mol dm^{-3} KCl).

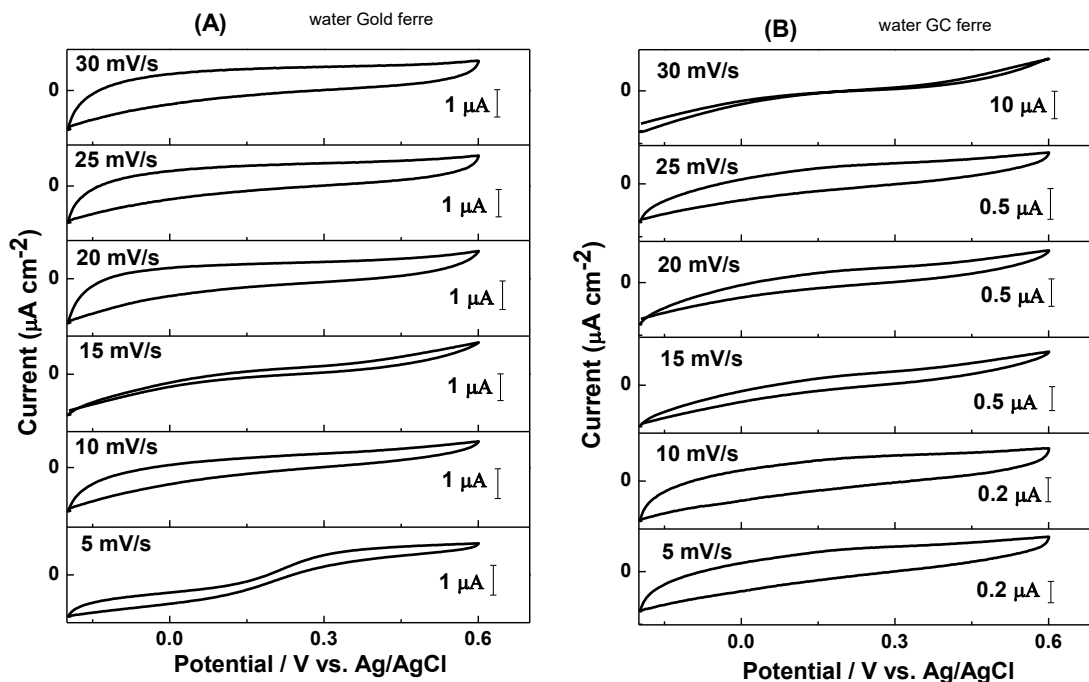


Figure 4. CV curves obtained for the modified electrodes after testing them in $20.0 \text{ mmol dm}^{-3}$ $\text{K}_3\text{Fe}(\text{CN})_6/\text{K}_4\text{Fe}(\text{CN})_6$ consisting of 0.1 mol dm^{-3} KCl vs Ag/AgCl (3.0 mol dm^{-3} KCl) at 20 mV s^{-1} (4 cycles). Each scan rate is linked to the scan rate used in the electropolymerisation process with $10.0 \text{ mmol dm}^{-3}$ 2NPPD in 10 mmol dm^{-3} neutral conditions vs Ag/AgCl (3.0 mol dm^{-3} KCl). (A) The 1.6 mm gold modified electrode ($A=0.0201 \text{ cm}^2$) and (B) the 3.0 mm modified glassy carbon electrode ($A=0.0707 \text{ cm}^2$).

Figure 5 highlights the absence of angle peaks for both types of electrodes used at a scan rate of 5 mV s^{-1} [17, 18]. The modified gold electrodes started to behave similarly to those in Figure 3 at a scan rate of 20 mV s^{-1} and above. The CVs experienced a drop in the current peak densities of $10 \mu\text{A}/\text{cm}^2$ at 5 mV/s and increased gradually up to $2000 \mu\text{A}/\text{cm}^2$ at 30 mV/s , whereas for the modified glassy carbon electrodes, CVs started to look similar to Figure 3 at a scan rate of 10 mV s^{-1} and above. The CVs experienced a drop in the current peak densities of $1 \mu\text{A}/\text{cm}^2$ at 5 mV/s and increased gradually up to $2000 \mu\text{A}/\text{cm}^2$ at 30 mV/s . This occurrence is related to the electropolymerisation of the 2NPPD monomer, as an insulating polymer layer was electrochemically formed at the surface of both electrodes' materials used. Similar observations were reported in our previous findings [13-19].

Figures 4 and 5 confirmed the deposition process of the polymer film on the electrode surface as per the method described previously [21]. The current researchers used the same method extensively and claimed this phenomenon was due to the passivation of the thin film deposition on the electrode's surface and hence electropolymerisation [13-19]. CV results showed that the electrode's surfaces were successfully coated and blocked by the polymer as the current peaks related to the bare electrodes diminished. Poly 2NPPD prepared from a neutral medium exhibited good passivation for both gold and glassy carbon electrodes.

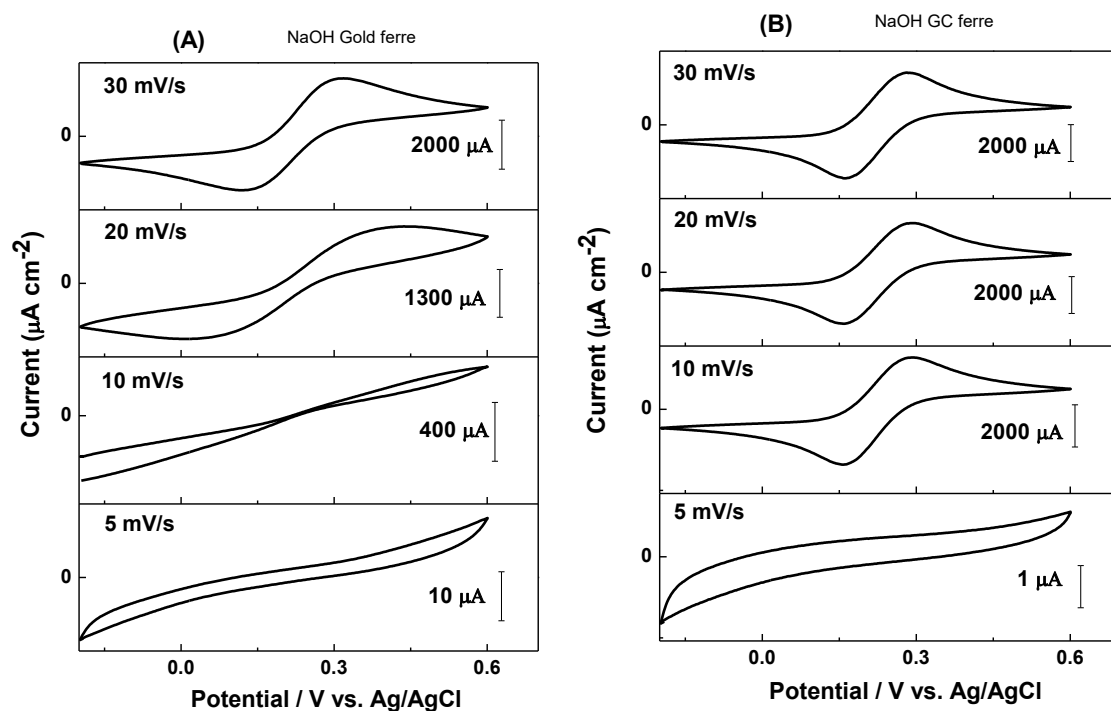


Figure 5. CV curves obtained for the modified electrodes after testing them in $20.0 \text{ mmol dm}^{-3}$ $\text{K}_3\text{Fe}(\text{CN})_6/\text{K}_4\text{Fe}(\text{CN})_6$ consisting of 0.1 mol dm^{-3} KCl vs Ag/AgCl (3.0 mol dm^{-3} KCl) at 20 mV s^{-1} (4 cycles). Each scan rate is linked to the scan rate used in the electropolymerisation process with $10.0 \text{ mmol dm}^{-3}$ 2NPPD in 10 mmol dm^{-3} caustic solutions vs Ag/AgCl (3.0 mol dm^{-3} KCl). (A) The 1.6 mm gold modified electrode ($A=0.0201 \text{ cm}^2$) and (B) the 3.0 mm modified glassy carbon electrode ($A=0.0707 \text{ cm}^2$).

Good passivation was also noted on the modified electrodes prepared from caustic aqueous solutions at 5 mV s^{-1} specifically. Hence, slow scan rates favoured electropolymerisation in caustic solutions, which could be attributed to the thickness of the polymer formed and thus, the amount of the polymer deposited on the surfaces [12].

Another factor to discuss here is the stability of the polymer formed in both solutions. The modified electrodes prepared using several scan rates from a neutral medium maintained their CV shape upon testing them in $20.0 \text{ mmol dm}^{-3}$ $\text{K}_3\text{Fe}(\text{CN})_6/\text{K}_4\text{Fe}(\text{CN})_6$, even when the CV cycles were extended up to 50 sweeps of potentials. This showed good stability of the polymer films formed in a neutral medium. In contrast, the modified electrodes prepared from caustic solutions were unable to maintain their CV shape and started to develop angle peaks after the second sweep of potentials, except for the modified electrodes prepared at a 5 mV s^{-1} scan rate.

Yu et. al. initially investigated several aqueous and non-aqueous solvents such as HNO_3 , HClO_4 , H_2SO_4 , CH_3CN , MeOH , dimethyl sulfoxide (DMSO), etc. for the electropolymerization of 4NoPD at the gold electrode [11]. However, the majority of these media gave difficulties relating to the low solubility of 4NoPD. They found that the poor solubility of 4NoPD monomer limits the ability to increase poly 4NoPD film thickness by increasing the concentration [11]. Similarly, the poor solubility of 2NPPD in different solvents limited us from increasing the monomer concentrations prior electropolymerisation.

However, it was found that the polymer formed is favoured to solubilise easily in caustic solutions. At the beginning of our experiments, we examined the electropolymerisation in 0.1 mol dm^{-3} NaOH. All the modified electrodes prepared from 0.1 mol dm^{-3} NaOH resulted in CV shapes of angle peaks upon testing in the $20.0 \text{ mmol dm}^{-3}$ $\text{K}_3\text{Fe}(\text{CN})_6/\text{K}_4\text{Fe}(\text{CN})_6$ solutions even those prepared from 1 to 5 mV s^{-1} . We subsequently decided to decrease the concentration of the caustic medium by 10-Fold up to 9.2 pH. The reason behind this was to find out whether or not the poly 2NPPD could be polymerised from caustic solutions. We tried to polymerise the poly 2NPPD at scan rates between 1 to 5 mV s^{-1} , which showed good stability towards the testing in the desired caustic solution medium. Above 10 mV s^{-1} scan rates, the polymer formed showed high solubility and hence, resulted in bad coverage of the electrode's surfaces. Therefore, the lower stability of the polymer in caustic solutions caused bad passivation of the modified electrodes.

Figure 6 illustrates the relationship of the first anodic current density versus the square root of the scan rates of the modified gold electrodes upon the electropolymerisation of $10.0 \text{ mmol dm}^{-3}$ 2NPPD in neutral and caustic solutions of NaOH. In the first CV cycle, the first anodic peaks that appeared in Figures 1A and 2A were used up to draw the plots in Figure 6. A linear relationship was obtained, and the correlation coefficient values were $R^2=0.9986$ for NaOH solution and $R^2=0.9994$ for the neutral medium with a zero intercept.

Figure 7 illustrates the relationship between the first anodic current density versus the square root of the scan rates of the modified glassy carbon electrodes for caustic sodium hydroxide solutions and neutral conditions. The first anodic peaks in Figures 1B and 2B were used to construct the plots. A linear relationship was obtained, and the correlation coefficient values were $R^2=0.9972$ for NaOH solution and $R^2=0.9977$ for neutral conditions with a zero intercept.

A linear dependence of the first peak current density versus the square root of the scan rates ($v^{1/2} \text{ s}^{-1/2}$) with a zero intercept was observed in Figures 6 and 7 for poly 2NPPD at scan rates ranging from 5 to 30 mV s^{-1} , providing evidence that the electrochemical reactions occur within the thin film on the electrode surface and not in solution [16, 22, 23]. Moreover, when the intercept is equal to zero, a decrease in the active sites on the working electrode during electropolymerisation occurred as the positive CV scans were employed. Therefore, the polymer thickness will build up and block more of the working electrode's surfaces [12]. These findings are in good agreement with Sayyeh et. al. [12]. They synthesised electrochemically poly(o-phenylenediamine-co-2-aminobenzothiazole) from an aqueous acid medium. They found that the peak current (i_p) increased linearly with the square root of the scan rate ($v^{1/2}$). They claimed that when the thickness of the polymer becomes thick, the diffusion of reactant inside the film becomes the slowest step then the process will be changed to diffusion transfer [12]. As noted in Figures 1 and 2, the first anodic peak disappeared in the subsequent cycles confirmed these observations.

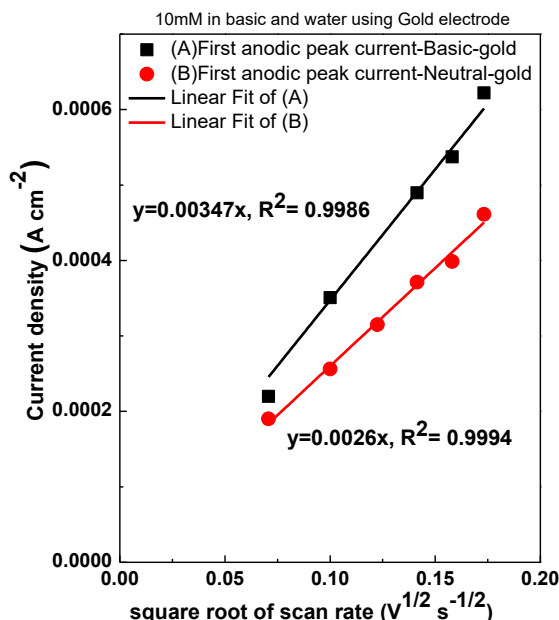


Figure 6. The first anodic current density vs the square root of the scan rates of the modified gold electrodes ($A=0.0201 cm^2$). The black line shows the first anodic peak current of $10.0 mmol dm^{-3}$ 2NPPD upon the electropolymerisation under caustic sodium hydroxide conditions and its corresponding linear fit ($R^2=0.9986$). The red line shows the first anodic peak current of $10.0 mmol dm^{-3}$ 2NPPD upon the electropolymerisation under neutral conditions and its corresponding linear fit ($R^2=0.9994$).

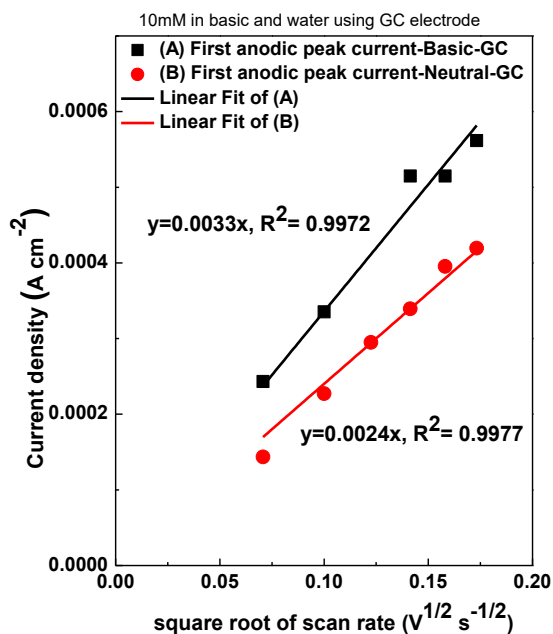


Figure 7. The first anodic current density vs the square root of the scan rates of the modified glassy carbon electrodes ($A=0.0707 cm^2$). The black line shows the first anodic peak current of $10.0 mmol dm^{-3}$ 2NPPD upon the electropolymerisation under caustic sodium hydroxide solutions and its corresponding linear fit ($R^2=0.9972$). The red line shows the first anodic peak current of $10.0 mmol dm^{-3}$ 2NPPD upon the electropolymerisation under neutral conditions and its corresponding linear fit ($R^2=0.9977$).

Table 4 presents the calculated diffusion coefficients (D) for the 2NPPD monomer. Data used to calculate D were obtained from the first cycle of the electropolymerisation CVs at different scan rates ranging from 5 to 30 mV s⁻¹. As the scan rate increased, the peak current (i_p) also increased linearly with the square root of the scan rate ($v^{1/2}$), confirming that the electropolymerisation of the 2NPPD monomer was a linear diffusion-controlled process. The diffusion coefficients were measured using the Randles–Sevcik Eq. 1: [24, 25]

$$I_p = (2.69 \times 10^5)n^{3/2}A\sqrt{D}\sqrt{v}C \dots \text{Eq. 1}$$

where, I_p is the peak current maximum in amps, n is the number of electrons in the event, A is the surface area of the working electrode in cm², D is the diffusion coefficient of the electroactive species in cm²/s, v is the scan rate of voltammograms in V/s, and C is the bulk concentration of the electroactive species mol/cm³.

Table 4. Calculated values of diffusion coefficients

Polymerization Medium	Diffusion Coefficients cm ² s ⁻¹ × 10 ⁻⁶	
	Gold electrode	Glassy carbon electrode
Neutral medium	0.93	0.80
Caustic medium	1.66	1.50

Table 4 shows that the D values calculated for the 2NPPD monomer prepared in neutral solutions were approximately similar for both gold and glassy carbon electrodes, 0.93 and 0.80 × 10⁻⁶ cm² s⁻¹, respectively. Similar observations were noted for caustic aqueous solutions, where D values were 1.66 and 1.50 × 10⁻⁶ cm² s⁻¹ for both gold and glassy carbon electrodes, respectively. The calculated D values for neutral solutions were lower than that for caustic aqueous solutions by approximately two folds. The calculated D value of 4NoPD monomer was 6.5 × 10⁻⁶ cm² s⁻¹ [26], whereas Sayyah et. al. the calculated D value of 7.0 × 10⁻⁶ cm² s⁻¹ of (1:1) molar ratio co-monomer of oPD and 2-aminobenzothiazole [12].

SEM micrographs of the bare gold-coated Si-chips and the modified (blocked) gold-coated Si-chips electrodes with poly 2NPPD are presented in Figures 8A and 8B, respectively. The bare gold surfaces were largely featureless. However, the surface morphology of the poly 2NPPD show agglomerated particles with faint scratches and look akin to tree-like structures. When comparing the morphological features to the bare electrodes, the poly 2NPPD surfaces showed large melted disordered patterns on the gold surfaces. Broad areas of distinct faint and dark irregular regions were also contained on gold electrode's surfaces.

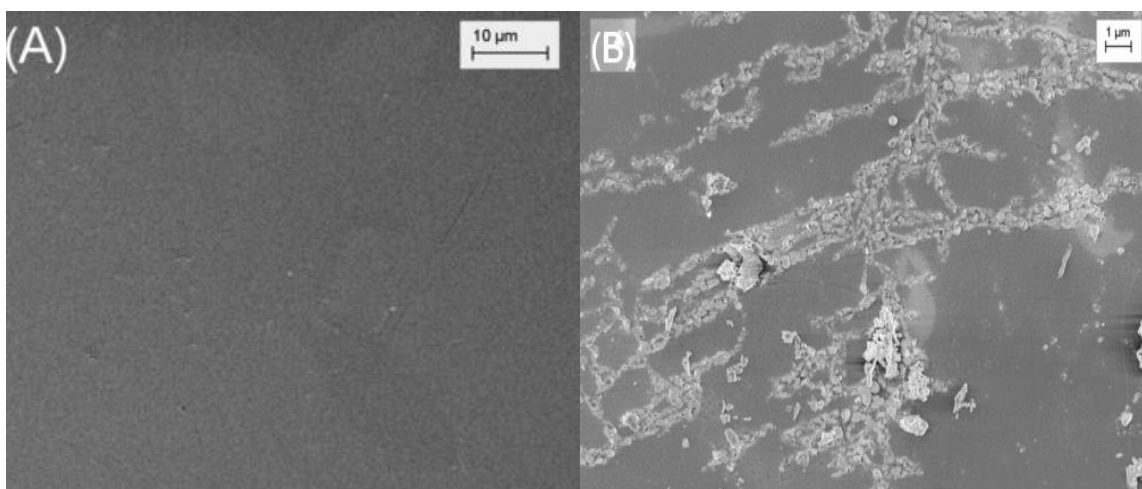


Figure 8. SEM images of gold-coated Si-chips ($A=1.0\text{ cm}^2$) of (A) the bare gold electrode at 1.00 KX magnification and (B) the blocked gold electrode at 5.00 KX magnification upon the electropolymerisation of 10 mmol dm^{-3} 2NPPD (0.1 mol dm^{-3} KCl) using CV vs Ag/AgCl at a 5 mV s^{-1} scan rate (25 cycles) in a neutral medium ($\text{pH}=7.0$).

The design of experiments empowered the model capabilities by providing statistical tools and necessary plots, such as a normal probability plot versus studentised residuals (Figure 9) and an interaction plot between the two studied factors (Figure 10).

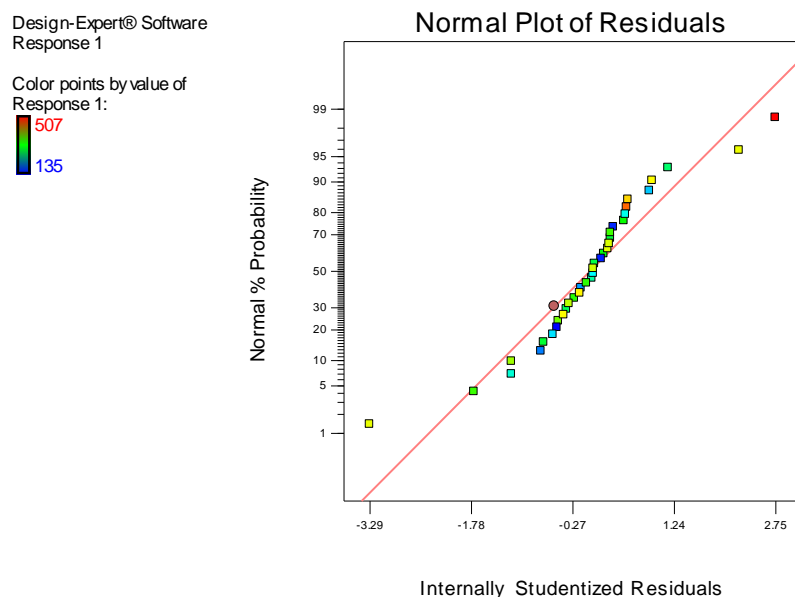


Figure 9. Normal probability vs studentised residuals for checking normality of residuals.

In Figure 9, the residuals normality plot resulted in a straight line with a normal distribution error. Hence, the normality assumption was valid for our proposed model. Moreover, data were distributed normally because the residuals were intensified approximately in the middle of the straight line and

showed no significant deviation from the residuals, which could be accepted as a pointer of outliers contained in this region.

Figure 10 presents the interaction plot of the electrode's material types versus the scan rate (mV s^{-1}) used in the electropolymerisation of $10.0 \text{ mmol dm}^{-3}$ 2NPPD prepared in neutral conditions at $\text{pH}=7.0$. The y-axis plots the response of the first anodic current peak densities (μAcm^{-2}). This figure further shows that the current densities increased proportionally as the scan rate increased. The upper level of all the factors obtained the greatest value. Figure 10 also illustrates the intersection of the two interaction lines at a 25 mV s^{-1} scan rate. The only interaction between the gold and glassy carbon electrodes upon the electropolymerisation of $10.0 \text{ mmol dm}^{-3}$ 2NPPD under neutral conditions at $\text{pH}=7.0$ was found at a 25 mV s^{-1} scan rate. Values of scan rates other than 25 mV s^{-1} on both electrodes resulted in parallel lines, indicating a lack of interaction among those factors [27].

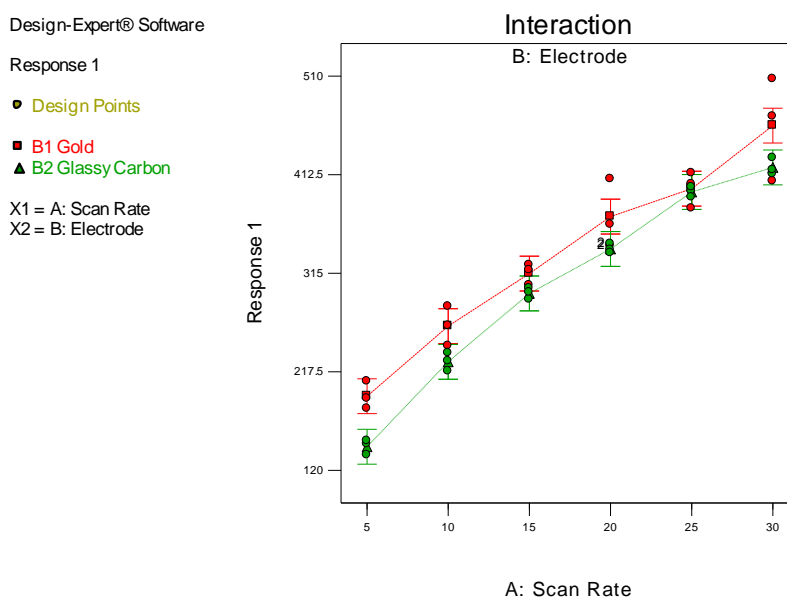


Figure 10. Interaction plot of the electrode type vs the scan rate (mV s^{-1}) in the electropolymerisation of $10.0 \text{ mmol dm}^{-3}$ 2NPPD under neutral conditions at $\text{pH}=7.0$. Response 1 is the first anodic current density in μAcm^{-2} . The types of electrodes used are gold electrodes ($A=0.0201 \text{ cm}^2$) marked in red and glassy carbon electrodes ($A=0.0707 \text{ cm}^2$) marked in green.

Table 5 presents the analysis of variance (ANOVA) of the partial sum of squares for the selected factorial model. ANOVA could be useful for the adequacy of the model. Using an F-test enables the estimation of the main and interaction effect degrees between factors. Table 5 lists the F-test and significance values, employed to test the overall model, the scan rate individual component (A), the electrode material type's individual component (B), and the interactions between AB.

The 67.98 F-value meant that the model was significant. Due to noise, there was only a 0.01% chance that a *Model F-Value* could occur. Values of *Prob > F* found to be less than 0.0500 indicate that the model terms were significant. In this case, A and B components are significant model terms. Values greater than 0.1000 indicate that the model terms are not significant.

Table 5. ANOVA table (partial sum of squares) for selected factorial model [Classical sum of squares – Type II]

ANOVA for selected factorial model						
Source	Sum of Squares	DF	Mean Square	F Value	p-value Prob > F	
Model	3.132×10 ⁵	11	28470.86	67.98	< 0.0001	significant
A-Scan Rate	3.029×10 ⁵	5	60572.25	144.63	< 0.0001	
B-Electrode	8250.69	1	8250.69	19.70	0.0002	
AB	2067.47	5	413.49	0.99	0.4460	
Pure Error	10051.33	24	418.81			
Cor Total	3.232×10 ⁵	35				

The following is the final equation in terms of coded factors regarding the response of the first anodic current peak densities:

$$\text{Response } (\mu\text{Acm}^{-2}) = + 318.42 - 150.08 * A[1] - 73.42 * A[2] - 13.58 * A[3] + 36.58 * A[4] + 78.58 * A[5] - 15.14 * B - 9.86 * A[1]B - 2.53 * A[2]B + 5.31 * A[3]B - 0.86 * A[4]B + 13.47 * A[5]B$$

It was noted that the predicted R² of 0.9300 was in reasonable agreement with the adjusted R² of 0.9547. In other words, adequate precision measures the signal to noise ratio. A ratio greater than 4 is desirable. The current model produced a ratio of 26.886, indicating that an adequate signal was obtained. In future studies, our model could be expanded to cover more factors or to navigate the design space.

Because the 2NPPD monomer has not been extensively studied in the literature, we conducted a comprehensive electrochemical study to enrich our knowledge regarding the electrochemical properties of the compounds. Therefore, a general factorial design was constructed and implemented through the electropolymerisation process of 2NPPD by CV in neutral medium in triplicate. The interactions between the operating parameters of the scan rates and the electrode's material types on the electropolymerisation of 2NPPD prepared in a neutral medium were examined. Poly 2NPPD prepared from a neutral medium exhibited good passivation for both gold and glassy carbon electrodes. Significance values, employed to test the overall model, the scan rate individual component, the electrode material type's individual component, and the interactions between them are significant model terms. The normality assumption was valid for our proposed model and data were distributed normally.

We proved that the electrochemical reactions occur within the thin film on the electrode surface and not in solution. Consequently, a decrease in the active sites on the working electrode during electropolymerisation occurred as the positive CV scans were employed. The current densities increased proportionally as the scan rate increased. An irreversible oxidation reaction obtained at both electrode surfaces. Therefore, the polymer thickness will build up and block more of the working electrode's surfaces. Morphological features of the poly 2NPPD show agglomerated particles with faint scratches similar to tree-like structures with melted disordered patterns. Broad areas of distinct faint and dark irregular regions were also observed.

The electropolymerisation of the 2NPPD monomer was a linear diffusion-controlled process. The CVs experienced a drop in the current peak densities, this occurrence is related to the electropolymerisation of the 2NPPD monomer, as an insulating polymer layer was electrochemically formed at the surface of both electrodes' materials used. For both gold and glassy carbon electrodes, the calculated D values for the 2NPPD monomer were approximately similar when prepared in neutral or caustic solutions. However, the calculated D values for neutral solutions were lower than that for caustic aqueous solutions by approximately two folds.

At slow scan rates, good passivation was also noted on the modified electrodes (gold and glassy carbon electrodes) prepared from caustic aqueous solutions. In caustic solutions, electropolymerisation was favoured at slow scan rates. Hence, it was attributed to the thickness, the amount of the polymer deposited on the surfaces, and to the stability of the polymer formed.

4. CONCLUSION

The current research successfully deposited thin polymeric films of 2-nitro-p-phenylenediamine (2NPPD) on gold and glassy carbon electrodes harvested from neutral (pH=7.0) and caustic aqueous solutions (pH=9.2). The poly 2NPPD films were developed in channels and showed a general morphology tree-like structure with agglomerated spherical particles as seen in the SEM micrographs.

In an investigation of 2NPPD electropolymerisation, the CV scans revealed a rapid drop in the anodic current peaks in neutral and caustic aqueous solutions. Further assurance of the modified electrode's surfaces coated with poly 2NPPD was conducted by running CV experiments in $K_3Fe(CN)_6/K_4Fe(CN)_6$ solutions. CV results showed that the electrode's surfaces were successfully coated and blocked by the polymer, as the current peaks related to the bare electrodes diminished. Poly 2NPPD prepared from a neutral medium exhibited good passivation for both gold and glassy carbon electrodes. We also noted good passivation on the modified electrodes prepared from caustic aqueous solutions specifically at 5 mV s^{-1} . Hence, the electropolymerisation in caustic solutions was favoured at slow scan rates. We refer to the thickness of the poly 2NPPD formed and hence, the amount of the polymer deposited on the surfaces by way of explanation. The calculated diffusion coefficients confirmed that the electropolymerisation of the 2NPPD monomer followed a linear diffusion-controlled process.

We conducted a general factorial design to understand the parameters affecting electropolymerisation. The normality assumption was valid for our proposed model. We also examined the relationship between the studied factors of scan rates along with the electrode's material types. Based on the interaction plots, the response of the first anodic current densities increased proportionally with scan rates. Despite observing an interaction at 25 mV s^{-1} , there were no interactions observed among any other studied factors. The model F-value was significant, and the predicted R^2 value was in reasonable agreement with the adjusted R^2 . An adequate precision signal to noise ratio was also achieved. Future studies could use our model to navigate the design space.

ACKNOWLEDGEMENTS

The authors are grateful to the College of Engineering at the University of Business and Technology (UBT), Jeddah, Saudi Arabia.

References

1. A.de Leon, R.C. Advincula, Chapter 11 - Conducting Polymers with Superhydrophobic Effects as Anticorrosion Coating, in: A. Tiwari, J. Rawlins, L.H. Hihara (Eds.) *Intelligent Coatings for Corrosion Control*, Butterworth-Heinemann, Boston, 2015, pp. 409-430.
2. P.S. Sharma, A. Pietrzyk-Le, F. D'Souza, W. Kutner, *Anal. Bioanal. Chem.*, 402 (2012) 3177-3204.
3. D. Akyüz, Ü. Demirbaş, A. Koca, F. Çelik, H. Kantekin, *J. Mol. Struct.*, 1206 (2020) 127674.
4. A. Rashti, J. Moncada, X. Zhang, C.A. Carrero, T.-S. Oh, *Mater. Chem. Phys.*, 231 (2019) 168-172.
5. Ş. Sağlam, A. Üzer, Y. Tekdemir, E. Erçağ, R. Apak, *Talanta*, 139 (2015) 181-188.
6. J. Arjomandi, H. Makhdomi, M.H. Parvin, *Synth. Met.*, 220 (2016) 123-133.
7. V.V. Shumyantseva, T.V. Bulko, L.V. Sigolaeva, A.V. Kuzikov, A.I. Archakov, *Biosens. Bioelectron.*, 86 (2016) 330-336.
8. C. Poochai, C. Sriprachubwong, N. Srisamrarn, J. Sudchanham, J.P. Mensing, T. Lomas, A. Wisitsoraat, A. Tuantranont, *J. Energy Storage*, 22 (2019) 116-130.
9. L. Ding, Q. Li, D. Zhou, H. Cui, R. Tang, J. Zhai, *Electrochim. Acta*, 77 (2012) 302-308.
10. S. Chemchoub, M. Elbasri, E.M. Halim, M. El Rhazi, *Mater. Today: Proc.*, 13 (2019) 720-729.
11. B. Yu, S.B. Khoo, *Electrochim. Acta*, 50 (2005) 1917-1924.
12. S.M. Sayyah, S.S. Abd El-Rehim, S.M. Kamal, M.M. El-Deeb, R.E. Azooz, *J. Appl. Polym. Sci.*, 119 (2011) 252-264.
13. A.S. Barham, B.M. Kennedy, V.J. Cunnane, M.A. Daous, *Electrochim. Acta*, 147 (2014) 19-24.
14. A.S. Barham, B.M. Kennedy, V.J. Cunnane, M.A. Daous, *Int. J. Electrochem. Sci.*, 9 (2014) 5389-5399
15. A.S. Barham, S. Akhtar, M.I. Alkhatib, S.Y. Jaradat, B.M. Kennedy, B. El Zein, *Materials Express*, 8 (2018) 305-315.
16. A.S. Barham, *Int. J. Electrochem. Sci.*, 13 (2018) 3660-3673.
17. A.S. Barham, *Int. J. Electrochem. Sci.*, 10 (2015) 4742-4751.
18. A.S. Barham, *J. New Mat. Electrochem. Syst.*, 18 (2015) 037-041.
19. A.S. Barham, *J. Electrochem. Soc.*, 162 (2015) G36-G40.
20. W. Richard, D. Evrard, P. Gros, *Int. J. Electrochem. Sci.*, 14 (2019) 453-469.
21. D.L. Franco, A.S. Afonso, S.N. Vieira, L.F. Ferreira, R.A. Gonçalves, A.G. Brito-Madurro, J.M. Madurro, *Mater. Chem. Phys.*, 107 (2008) 404-409.
22. M. Quinto, S.A. Jenekhe, A.J. Bard, *Chem. Mater.*, 13 (2001) 2824-2832.
23. M.T. Hsieh, T.J. Whang, *J. Electroanal. Chem.*, 795 (2017) 130-140.
24. J.E.B. Randles, *Trans. Faraday Soc.*, 44 (1948) 327-338.
25. A. Sevic, *Collect. Czech. Chem. Commun.*, 13 (1948) 349-377.
26. K. Yip, K.Y. Tam, K.F.C. Yiu, *J. Chem. Inf. Comput. Sci.*, 37 (1997) 367-371.
27. P. García-Manrique, M.B. González-García, M.C. Blanco-López, Chapter 35 - Design of experiments at electroanalysis. Application to the optimization of nanostructured electrodes for sensor development, in: M.T. Fernandez Abedul (Ed.) *Laboratory Methods in Dynamic Electroanalysis*, Elsevier, 2020, pp. 361-371